Journal of the Chinese Society of Mechanical Engineers, Vol.46, No.6, pp569~577 (2025)

Binocular Stereo Vision Measurement System with Novel Edge-Enhancement Feature Algorithm for Electric Vehicle Battery Modules

Shu-Zhe Chen *, Wei-Hong Lim *, Chien-Sheng Liu **,
Hua-Bin Lee ***, Chien-Jung Liao *** and Ming-Fu Chen ****

Keywords：Binocular stereo vision, High-precision 3D measurement, Localization error, Image processing, 3D scanning.

ABSTRACT

In this study, a binocular stereo vision measurement system with novel edge-enhancement feature algorithm is proposed for the electrode circular hole array position in electric vehicle battery modules. A simulated workpiece of the electrode circular hole array in an electric vehicle battery module has been created for testing. The proposed system combines image processing techniques with a novel edge-enhancement feature algorithm to identify the features of circular hole arrays in the workpiece and performs three-dimensional point coordinates reconstruction of the feature centers. The proposed system is capable of measuring at a distance of 215 mm from the workpiece and has a measurement range of 450 mm × 200 mm, size of electric vehicle battery modules, which can be increased by using stitching process. The experimental results show that 3D points with a measuring accuracy of 0.1 mm and measuring repeatability of 0.03 mm can be achieved.

INTRODUCTION

High precision measurement and compensation technology are becoming increasingly crucial in reducing errors and enhancing product quality. One major challenge in the manufacturing and assembly process is the errors left by workpieces, making automation difficult. The industry now requires not only expanded capacity, but also increased precision and strength in component processing and assembly. By measuring and compensating for these errors, automated production and processing can be achieved. Localization error measurement is crucial in industrial production and automation, as it determines the precision and quality of machined products. As more traditional industries shift to automated production, several issues emerge, including the need to replace human-operated machinery with robots, eliminate assembly errors, and account for component errors (Liu et al., 2019; Huang et al., 2012). Accurately measuring and compensating for errors can increase the precision and cost-effectiveness of the automated manufacturing process (Chen et al., 2018), resulting in higher-quality products. In the past, the standard approach for measuring errors used a coordinate measuring machine (CMM), which provides excellent resolution and precision. However, this method is time-consuming, inefficient, and posed a risk of causing scratches on the object's surface. It is also unsuitable for measuring soft components. As a result of these limitations, non-contact optical scanning techniques (Flores-Fuentes et al., 2023), such as binocular stereo vision, structured light (Huang et al., 2012; Liu et al., 2023), and time-of-flight (M. A. Isa and I. Lazoglu, 2017), have been introduced as alternatives. These methods are faster and less constrained, and they also prevent surface contact.

Recently, due to environmental issues, the electric vehicle market has been increasing year by year. Therefore, the relevant processes of the electric vehicle battery module have received attention from the automotive industry. Among them, laser welding technology with a robotic arm for electric vehicle battery modules is widely applied. In the laser welding process of electric vehicle battery modules, the detection of the electrode circular hole array position in the electric vehicle battery module is crucial.

Paper Received December, 2024. Revised April, 2025. Accepted April, 2025. Author for Correspondence: Chien-Sheng Liu

* *Graduate Student, Department of Mechanical Engineering, National Cheng Kung University, Tainan 70101, Taiwan, ROC.*

***Professor, Department of Mechanical Engineering, National Cheng Kung University, Tainan 70101, Taiwan, ROC.; Academy of Innovative Semiconductor and Sustainable Manufacturing, National Cheng Kung University, Tainan 70101, Taiwan, ROC.*

*** *Yulon Motors Co., Ltd., Miaoli County, Taiwan, ROC.*

**** *National Center for Instrumentation Research, National Institutes of Applied Research, Hsinchu, Taiwan, ROC.*

Because accurate positions of electrode circular hole arrays are necessary for automated laser welding. If the positions of the electrode circular hole arrays are incorrect, the quality of the automated laser welding for it will be affected. However, due to the large size and high surface reflectivity of electric vehicle battery modules, the difficulty of automated measurement has increased. The motivation of this study is to address this issue and propose a binocular stereo vision measurement system for the electrode circular hole array position in electric vehicle battery modules.

Binocular stereo vision is used in this study due to its lower cost, improved accuracy, and its ability to overcome metal surface reflection using image processing techniques. Here, some literature on binocular stereo vision is reviewed. Luo et al. (2017) proposed a binocular stereo vision system for automatically locating the position and posture of the workpiece, with background subtraction and foreground edge line extraction designated for positioning. However, the proposed image processing method is still having difficulty accurately detecting all contour lines, resulting in the absence of certain feature points. Han et al.(2022) proposed a stereo vision system for large workpiece localization. The method reconstructed the 3D positions of the markers using designated markers and a novel stitching process. The iterative closest point (ICP) algorithm was employed to integrate the reconstructed positions of the markers into one whole part. However, these markers needed to be attached to the workpiece, which makes the method unsuitable for large-scale measurements in real-world manufacturing lines. Zhu et al. (2022) proposed an active imaging perception and target measurement method that combines laser scanning and binocular vision. Laser lines scanned to the target provided strong characteristics of binocular matching to enhance anti-interference. However, the precision of measuring the target using the fully reconstructed point cloud is poor, and the point cloud processing takes a longer time.

To reconstruct their three-dimensional coordinates, the majority of approaches for measuring errors using stereo vision technology rely on the localization of local feature points. These coordinates are then utilized for further measurements, such as point-to-point distance and the relative distance or posture between reference coordinates. In an effort to reduce errors when identifying feature points, some researchers employed self-made markers or detected corner points on checkerboards as feature points. Unfortunately, this method proves inefficient for large-scale measurements. This study improves upon previous research by incorporating multiple sets of stitching and a novel edge-enhancement feature algorithm, resulting in a system with improved accuracy and large scanning range.

MEASUREMENT PRINCIPLE AND SYSTEM ARCHITECTURE

Measurement Principle

Binocular stereo vision is a passive 3D scanning technique that mimics the human visual system by employing two cameras to observe the same object at the same time (Taryudi and M. S. Wang.2018). Unlike other methods, binocular stereo vision could perform scanning under normal lighting conditions without the use of additional illumination equipment. The key principle of binocular stereo vision is disparity, which is the difference in the imaging positions of the object in each camera due to the differing placements of the two cameras. By employing the disparity relationship, precise computations of the object's depth and position in space become achievable, allowing for the accurate reconstruction of three-dimensional objects.

A binocular stereo vision system begins with the capture of images from two distinct view cameras. After image processing, which includes camera calibration, feature points are detected and described in the images (Hartley et al., 2004). To obtain three-dimensional depth information, disparity is calculated using these points and stereo matching is performed. The process flowchart of binocular stereo vision is depicted in Fig. 1.

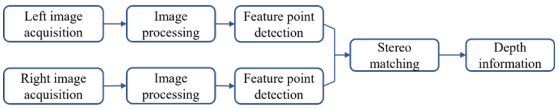

Fig. 1. Process flowchart of fundamental binocular stereo vision.

Image acquisition is critical for binocular stereo vision. More information allows for better results, so practical applications consider factors such as field of view, illumination, camera performance, and scene characteristics (Cyganek and Siebert, 2009). Image processing techniques like contrast enhancement and smoothing can be used to reduce noise and distortion. Camera calibration corrects distortion and establishes geometric relationships for accurate depth calculations. Feature point detection extracts unique points in an image, such as corners and edges. Corners are more easily obtained and precise, making them ideal for calibration. Edges are more difficult to obtained due to their irregularities and may require point subset detection and connection before they can be used as features (R. Maini and H. Aggarwal, 2009). Stereo matching creates a disparity map by establishing correlation between locations in various images. Stereo matching algorithms are classified into three types: feature-based, area-based, and phase-based. Feature-based algorithms use descriptors of matched points to find correspondences (Lowe, 2004). Area-based algorithms find similar regions between images (Wang and Zheng, 2008). Phase-based algorithms project patterns onto the images and then match the

patterns to find correspondences (Li et al., 2010). Although phase-based algorithms are generally more precise than feature-based or area-based algorithms, they are affected by reflections.

Epipolar Geometry

Epipolar geometry is a geometric model that describes the relationship between two images of the same scene taken from different viewpoints. It is used to align two images before disparity evaluation, which is a process of measuring the differences in the position of corresponding points in the two images. These differences, known as disparities, can be used to reconstruct the 3D coordinates of the points in the scene (Zhang, 1998). The model is based on the camera internal parameters and relative positions of two cameras. The model allows us to find the corresponding points in the two images, which can then be used to reconstruct the 3D coordinates of the points in the scene.

The process of 3D reconstruction is known as multi-view geometry. The object is captured from several perspectives in this method to obtain different sets of point cloud data. The point clouds' overlapping regions are then matched by computing the Euclidean distance between feature point positions in different images (Yang et al., 2018). The point clouds are rotated and translated using transformation matrices before being merged into the same coordinate system to create an accurate 3D point cloud of the object.

System Architecture

In this study, the proposed binocular stereo vision measurement system, as shown in Fig. 2, includes two CMOS cameras with suitable lenses and one calibration board to calibrate the system.

A chessboard calibration board is used in this study to improve the accuracy of corner point detection through sub-pixel refinement. The Imaging Source DFK 33UX226 cameras with Sony IMX226CQJ CMOS sensors are employed for their excellent imaging capabilities. Moritex ML-M0625UR lenses are used to achieve the desired measurement range. The specific configuration is listed in Table 1.

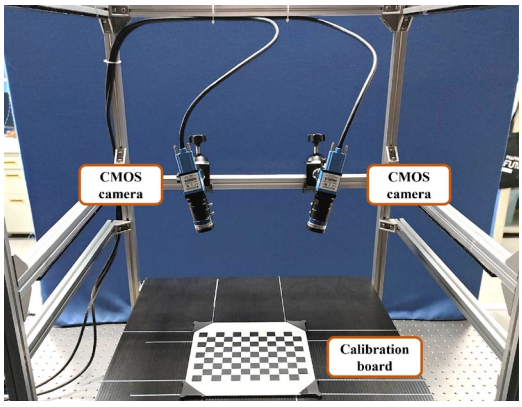

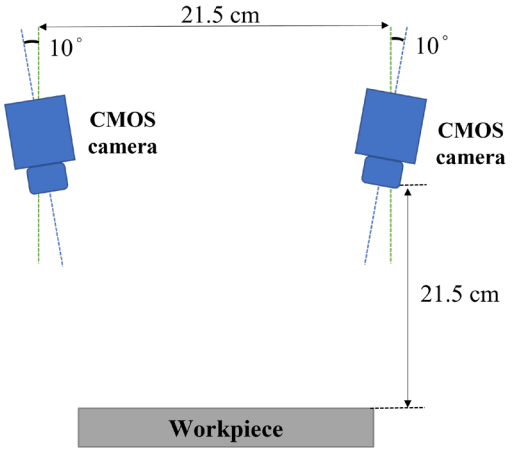

Fig. 2. Architecture of proposed binocular streo vision measurement system.

Table 1. Specific configuration of proposed system.

Item	Model	Specification
CMOS camera	The Imaging Source DFK 33UX226	Resolution: 3000 × 4000 (12MP) Sensor type: Sony IMX226CQJ CMOS TARVIS rolling shutter Sensor size: 1/1.7” Pixel size: 1.85 µm × 1.85 µm Max frame rate: 30 fps
Lens	Moritex ML-M0625UR	Focal length: 6 mm Focal ratio (Fno): 2.5 – 16 Angle of view: 74.5° × 57° Minimum working distance: 100 mm
Checkerboard calibration board	Custom	Pattern size: 180 mm × 135 mm Pattern array: 12 × 9 Square side length: 15 mm Accuracy: 0.01 mm

First, the binocular stereo vision system was calibrated to obtain camera calibration parameters and camera models. Then, the left and right images of the object are inputted and undistorted using the calibration parameters. Rectification is applied to ensure that corresponding points in the left image can be found on the same horizontal axis in the right image, with the two image planes placed parallel to each other. Subsequently, image processing techniques were used for feature extraction. The features were matched to generate three-dimensional point cloud coordinates (Lin et al., 2020).

MATHEMATIC MODEL OF BINOCULAR STEREO VISION SYSTEM

Camera Imaging Model

Imaging an object in three-dimensional space onto a screen is a complex process that involves multiple coordinate transformations. The pinhole imaging model, a fundamental concept in optics and camera imaging, is often used to simplify this process, as shown in Fig. 3.

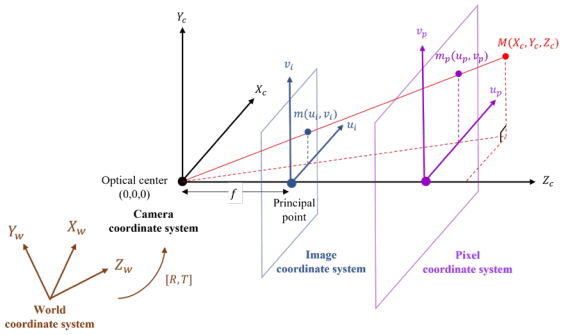

Fig. 3. Pinhole imaging model.

The pinhole imaging model provides a simplified representation of how a camera captures images. It divides the camera's parameters into two categories: intrinsic and extrinsic. The intrinsic parameters describe the geometric characteristics of the camera, such as focal length, principal point, and lens distortion. The extrinsic parameters describe the relative position and rotation angles between the camera coordinate system and the world coordinate system (Huang et al., 2021).

A space coordinate $\mathbf{M}_w(X_w, Y_w, Z_w)$ in world coordinate system undergo rigid transformation to camera coordinate system $\mathbf{M}(X_c, Y_c, Z_c)$. Then, $\mathbf{M}$ transformed to image coordinate system $\mathbf{m}(u_i, v_i)$ by perspective projection. Finally, $\mathbf{m}$ is converted to pixel coordinate system $\mathbf{m}_p(u_p, v_p)$ which represented the position of the point in the pixel grid of an image.

In practical imaging, cameras are typically equipped with lenses to capture external images. However, lens manufacturing and assembly are not perfect, leading to various types of nonlinear distortions in the camera image. Thus, a linear camera model cannot accurately describe the geometric relationship of camera image. To eliminate the influence of distortions on the camera model, the distortion model proposed by Brown (Brown, 1971) is widely used in computer vision. This model incorporates two significant distortions that affect the projection in the image which are radial distortion and tangential distortion.

3D Point Stitching Process

The ICP algorithm is widely used in 3D point cloud registration. It facilitates rigid transformation, including rotation and translation, between point clouds while preserving the original three-dimensional information (Arun et al., 1987; Besl and McKay, 1992). One of the significant advantages of the ICP algorithm is its ability to work directly on the raw point cloud data, eliminating the need for prior segmentation or feature extraction. Additionally, when a good initial alignment is given, the ICP algorithm exhibits high accuracy and convergence, resulting in precise point cloud registration. It is generally more suitable for applications where the number of point clouds is relatively small, such as the proposed system in this study.

In ICP algorithms, data from two point clouds were defined as $P = \{p_1, p_2, p_3, \cdots, p_n\}$ and $Q = \{q_1, q_2, q_3, \cdots, q_n\}$. To align the point cloud Q to point cloud P with rigid transformation, 3×3 rotation matrix $\boldsymbol{R}_{\mathrm{pc}}$ and 3×1 translation matrix $\boldsymbol{T}_{pc}$ were established. The relationship between two point clouds can be expressed as follows:

$$q_i = \boldsymbol{R}_{pc} p_i + \boldsymbol{T}_{pc} \tag{1}$$

where i is the number of points in a point cloud. As it is an ideal transformation that aligns point cloud Q to point cloud P, so the optimal solutions of the rotation matrix $\boldsymbol{R}_{pc}^*$ and translation $\mathbf{T}_{pc}^*$ must be solved to minimize the discrepancy between the two point clouds. Suppose D as the optimal function of $\boldsymbol{R}_{pc}^*$ and $\mathbf{T}_{pc}^*$, the function can be expressed with:

$$D_{(\boldsymbol{R}_{pc}^*, \boldsymbol{T}_{pc}^*)} = \underset{\boldsymbol{R}_{pc}, \boldsymbol{T}_{pc}}{argmin} \sum_{i=1}^{n} \left\| q_i - \boldsymbol{R}_{pc} p_i - \boldsymbol{T}_{pc} \right\|^2 \tag{2}$$

Singular value decomposition (SVD) algorithm is used to determine the best-fit transformation. First, center of mass of two point clouds was defined as:

$$\mu_p = \frac{1}{n} \sum_{i=1}^{n} p_i, \qquad \mu_q = \frac{1}{n} \sum_{i=1}^{n} q_i \tag{3}$$

By substituting the obtained centers of mass into Eq. (2), Eq. (2) can be written as:

$$D_{(\boldsymbol{R}_{pc}^{*},\boldsymbol{T}_{pc}^{*})} = \underset{\boldsymbol{R}_{pc},\boldsymbol{T}_{pc}}{argmin} \sum_{i=1}^{n} \left(\left\| q_i' - \boldsymbol{R}_{pc} p_i' \right\|^2 + \left\| \mu_q - \boldsymbol{R}_{pc} \mu_p - \boldsymbol{T}_{pc} \right\|^2 \right) \quad (4)$$

where $p_i' = p_i - \mu_p$, $q_i' = q_i - \mu_q$. From Eq. (4), optimal $\boldsymbol{R}_{pc}^{*}$, $\mathbf{T}_{pc}^{*}$ can be solved. The expression of the two matrices is as follows:

$$\begin{aligned} \boldsymbol{R}_{pc}^{*} &= \underset{\boldsymbol{R}_{pc}}{argmin} \sum_{i=1}^{n} \left\| q_i' - \boldsymbol{R}_{pc} p_i' \right\|^2 \\ &= \underset{\boldsymbol{R}_{pc}}{argmin} \sum_{i=1}^{n} -q_i'^{T} \boldsymbol{R}_{pc} p_i' \\ \boldsymbol{T}_{pc}^{*} &= \mu_q - \boldsymbol{R}_{pc} \mu_p \end{aligned} \quad (5)$$

Finally, by substituting the obtained optimal rotation matrix $\boldsymbol{R}_{pc}^{*}$ and translation matrix $\mathbf{T}_{pc}^{*}$ from Eq. (5) into Eq. (1) for $\boldsymbol{R}_{pc}$ and $\boldsymbol{T}_{pc}$, respectively, two point clouds can be aligned.

The relative transformation matrix was calculated using the 3D coordinates of duplicate features during the 3D stitching procedure. However, the proposed system has a smaller measurable range than the simulated workpiece of the actual electric vehicle battery module in order to maintain high accuracy [25]. Therefore, in this study, the test workpiece was moved to capture the entire length of the simulated workpiece under test. The assumption underlying this method is that the precision of the single set of binocular vision measurements must be good. The feature center's 3D coordinates, specifically from points 5 to 8, are reconstructed and incorporated into the 3D stitching process. The point clouds can be reconstructed to represent the whole size of the workpiece using the stitching process, as shown in Fig. 4.

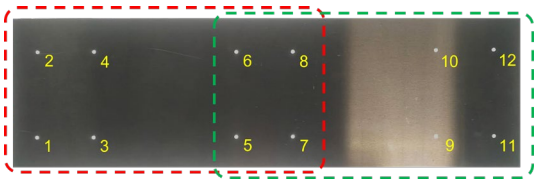

Fig. 4. Example of 3D point stitching process.

NOVEL EDGE-ENHANCEMENT FEATURE ALGORITHM

Due to machining and assembly errors, the shape of the electrode circular holes may not be perfect cylindrical holes, and there are often burrs or defects around the cylindrical holes, increasing the difficulty of machine vision. According to our experiences, the conventional feature detection approaches cannot satisfy the required measuring accuracy 0f 0.1 mm. To enhance the accuracy of the features of the electrode circular hole array extracted from the simulated workpiece of the electrode circular hole array in an electric vehicle battery module, this study proposes a novel edge-enhancement feature algorithm based on image processing and morphology techniques. The process begins by applying the region-of-interest (ROI) technique to mask the input image, thereby focusing the processing on relevant areas and improving efficiency. Subsequently, the image is converted to grayscale and dynamically binarized using the Canny algorithm. The properties of the regions in a binary image, including area, major axis length, eccentricity, solidity, and extent, are analyzed and filtered to select the regions corresponding to the features. Following this, hole-filling and closing operations are applied to the filtered feature regions, further optimizing and refining them, reducing noise, and filling any gaps or holes that may exist.

Since the initial feature regions might still contain noise or holes resulting from uneven illumination or the binarization threshold, further refinement is achieved through edge detection. The binary image obtained from the region properties filter is subjected to erosion, and the eroded image is subtracted from the edges detected in the original image. Through the "AND" operation, the resulting image is combined with the dilated feature regions, producing a circular pattern that outlines the edges of the features. Ultimately, a closing operation is applied to the resulting edges to achieve more precise and well-defined feature regions. The novel edge-enhancement feature algorithm proposed in this study, depicted in Fig. 5, enhances the visibility and accuracy of the image's features, leading to a more dependable representation of the workpiece.

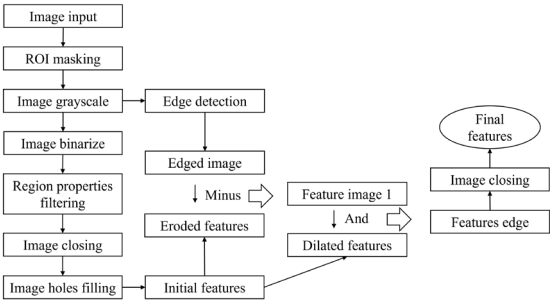

Fig. 5. Improved edge-enhancement feature algorithm.

Fig. 6 presents experimental image showing various stages of the original image, edged image, initial features, eroded features, feature image 1, dilated feature, features edge, and image closing processing. Fig. 7 compares the results of image processing of conventional region properties filter and proposed edge-enhancement algorithm. The identified edges are displayed as white lines, while the authentic features are highlighted in red color, following two stages of image processing. The results indicate that

the features of the electrode circular holes are successfully extracted from the original images, unaffected by defects.

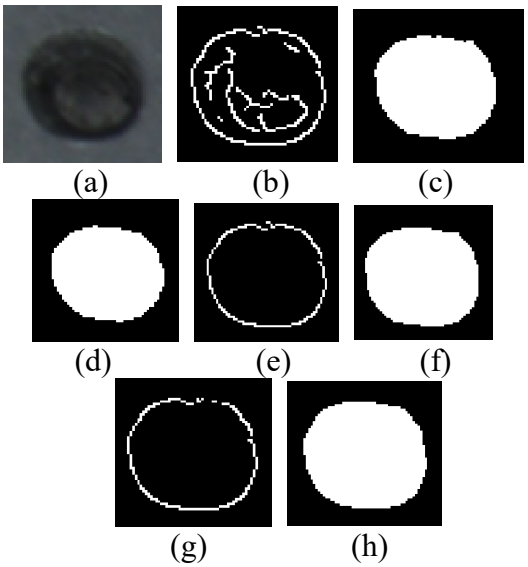

Fig. 6. Image processing results: (a) original image, (b) edged image, (c) initial features, (d) eroded features, (e) feature image 1, (f) dilated feature, (g) features edge, and (h) image closing processing.

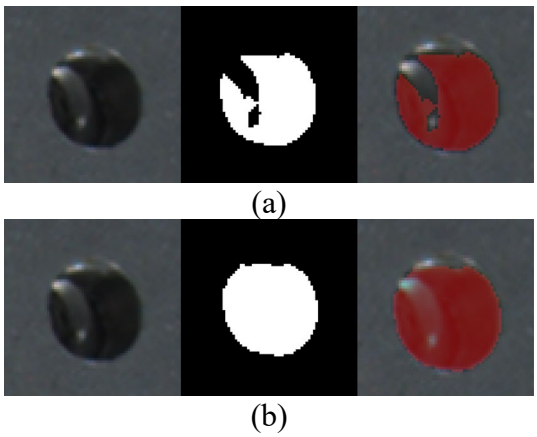

Fig. 7. Results of image processing: (a) feature after region properties filter and (b) feature after edge-enhancement algorithm.

EXPERIMENTAL RESULTS

Accuracy Evaluation

In this section, field measurements are assessed to establish the absolute accuracy of the proposed system. For accuracy evaluation, a standard circle grid board was utilized, as illustrated in Fig. 8. The circle detection employs the edge-enhancement feature algorithm proposed in this study. Subsequently, the centers of the circles were re constructed in 3D space once they were detected on the circle grid board. The distances between the centers (both horizontally and vertically) were measured, as the actual value between them is 10 mm. The outcomes are illustrated in Fig. 9. The average distance measures 10.0068 mm, with a standard deviation of 0.0023 mm.

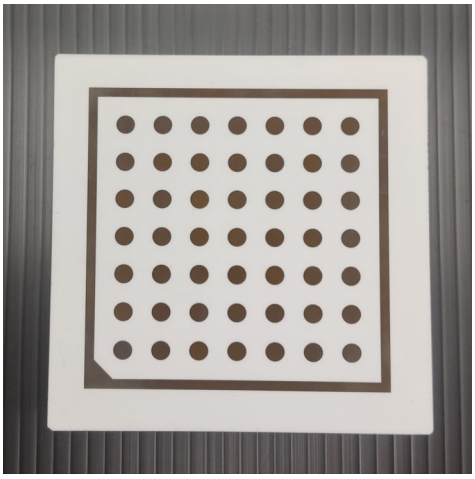

Fig. 8. Circle grid board.

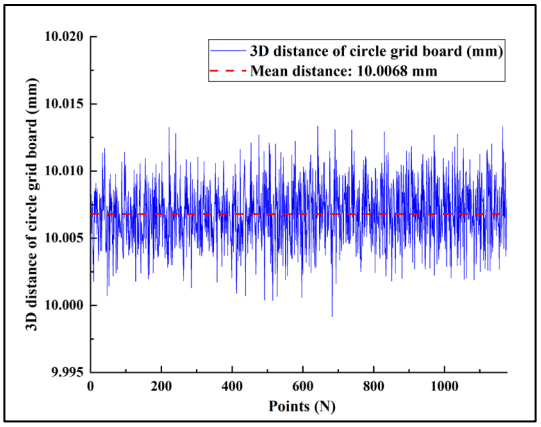

Fig. 9. 3D distance of generated point from circle grid board.

Evaluation of Test Workpiece For Real Application Field

The proposed binocular stereo vision measurement system is aimed to measure the electrode circular hole array position in electric vehicle battery modules. Due to commercial confidentiality, a test workpiece of the electrode circular hole array in an electric vehicle battery module has been created for testing in this study [24]. To ensure compatibility, a material with comparable properties, such as high reflectivity, was selected. In order to replicate the battery modules, the dimensions of the test workpiece were set at 400 mm × 135 mm, incorporating a 12-feature hole array as illustrated in Fig. 10. The required measuring accuracy is ≤ 0.1 mm, aligning with the demands of commercial applications.

Fig. 10. Test workpiece with 12-feature hole array.

Repeatability Measurement

Repeatability showcases the reliability of a system when measuring the same position multiple times using the same measurement procedure. Several sets of data were collected by conducting repeated measurements on the simulated workpiece. These datasets are employed to compute the system's average measurement value, and each dataset is individually compared to this average value. This analysis enables the assessment of the system's stability and consistency, which forms a crucial basis for system calibration and optimization. Five sets of data were gathered for analysis, and the 3D coordinates of the feature holes were computed. These coordinates were subsequently averaged across the five measurements. Distances between the axes were assessed individually, along with absolute distances in 3D space. The outcomes of the repeatability assessment are presented in Fig. 11. The experimental results show that the measuring repeatability of the proposed system is smaller than 0.03 mm.

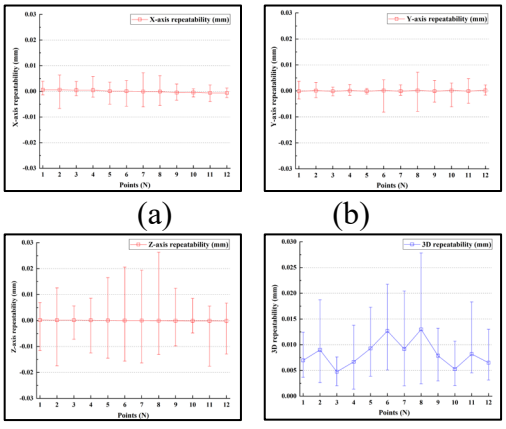

Fig. 11. Repeatability of experiments: (a) in X-axis direction; (b) in Y-axis direction; (c) in Z-axis direction; (d) in 3D space.

Comparison with Commercial System's Results

After conducting accuracy and repeatability analyses, the data acquired from our repeatability measurements is contrasted with those obtained from the commercial 3D scanning system, GOM Atos Core 300, which asserts a 0.02 mm accuracy. As explained in the process of 3D point stitching, the ICP technique is employed to align the dataset from our proposed system. The error of our system is calculated using the absolute distance between corresponding points in the two datasets. The outcomes of the distance error assessment are displayed in Fig. 12.

In this study, GOM Atos Core 300 served as a reference standard for our system. While this approach may promise enhanced accuracy, certain disparities emerged. For instance, Atos Core 300 utilized structured light scanning, whereas our workpiece featured a highly reflective metal surface, potentially influencing the accuracy of the structured light scanning mechanism. Powder coating was implemented to mitigate light reflection. Additionally, slight variations in ambient conditions between Atos Core 300 and our system setup existed, which could introduce measurement uncertainty. The experimental results show that the measuring accuracy of the proposed system is smaller than 0.1 mm.

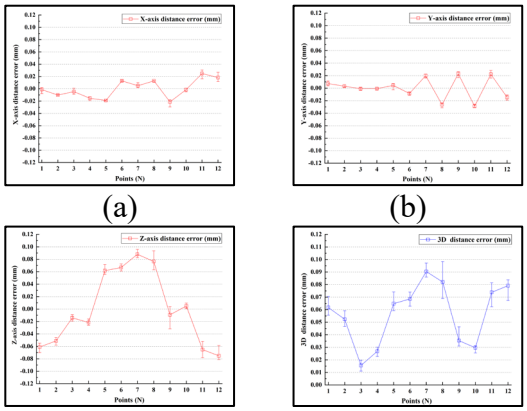

Fig. 12. Distance error comparison with GOM Atos Core 300: (a) X-axis direction; (b) Y-axis direction; (c) Z-axis direction; (d) 3D space.

Comparison with other feature detection methods' results

In the preceding section, 3D coordinates were reconstructed through the utilization of the proposed edge enhancement algorithm. To compare the outcomes of 3D coordinate reconstruction in terms of repeatability and 3D distance error with those of GOM Atos Core 300, two feature detection approaches were selected. "Find circle" employed the circle Hough transform to identify circles in the image [25]. K-medoids, a clustering method [26], was used to assess the 2D coordinates of feature centers following the application of region properties filtering to a binary image. The results indicated that the proposed feature detection method significantly enhances the measuring repeatability and accuracy of 3D coordinate reconstruction, as depicted in Fig. 13. The 3D reconstruction error of the feature points is below 0.1 mm, which also proves that the stitching process has not introduced any significant bias.

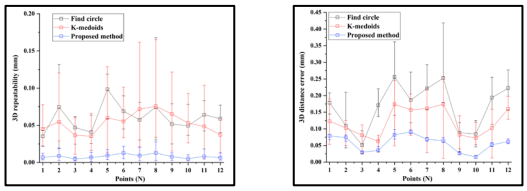

(a) (b)

Fig. 13. Comparison with other feature detection methods' results: (a) repeatability; (b) 3D distance error.

System Efficiency Analysis

Although accuracy is the core indicator of this research, system efficiency remains a critical consideration for industrial applications. Based on the current hardware configuration and algorithmic workflow, a single local measurement (including image capture, feature processing, and 3D reconstruction) can be completed within 300 ms. Full-scale measurements for a 450 mm × 200 mm area require multiple local scans and stitching, with a total processing time of approximately 800 ms. This efficiency meets the requirements of most production line cycle times. However, to achieve a further improvement to millisecond-level response times, hardware acceleration can be employed by porting the image processing algorithm to a GPU or embedded FPGA. This is expected to reduce feature processing time to under 20 ms. Additionally, for fixed workpiece geometries, pre-storing ROI templates can reduce the computational load of dynamic binarization.

CONCLUSION

This study proposes a binocular stereo vision measurement system with an edge-enhancement feature algorithm designed to precisely locate the electrode circular hole array position in electric vehicle battery modules. A prototype was built, and a series of experiments were conducted to verify the performance of the proposed system. Although the proposed system is initially positioned at a height of 215 mm above the target object, the utilization of point cloud stitching significantly extends the measurement range to 450 mm × 200 mm. The experimental results show that the proposed system achieves a measuring accuracy of 0.1 mm with relative errors of 0.022% and a measuring repeatability of 0.03 mm, satisfying the required accuracy. The proposed method effectively avoids the influence of workpiece reflection, providing a solution that preserves scanning accuracy for the automated laser welding process of electric vehicle battery module. Its modular architecture allows for expansion to measure different materials (such as composites and plastics) and geometric features by adjusting algorithm parameters and optimizing hardware configurations.

ACKNOWLEDGMENT

The authors gratefully acknowledge the financial support provided to this study by [details omitted for double-anonymized peer review].

DECLARATION OF CONFLICTING INTERESTS

The author(s) declared no potential conflicts of interest with respect to the research, authorship, and/or publication of this article.

REFERENCES

Arun, K. S., Huang, T. S., and Blostein, S. D., "Least-Squares Fitting of Two 3-D Point Sets," *IEEE Trans. Pattern Anal. Mach. Intell.*, vol. PAMI-9, no. 5, pp. 698-700, 1987.

Besl, P. J. and McKay, N. D., "A Method for Registration of 3-D Shapes," *IEEE Trans. Pattern Anal. Mach. Intell.*, vol. 14, no. 2, pp. 239-256, 1992.

Brown, D., "Close-Range Camera Calibration," *Photogramm. Eng.*, vol. 37, no. 8, pp. 855-866, 1971.

Chen, L. C., et al., "A Novel Feature Detection Method Using Multi-Dimensional Image Fusion for Automated Optical Inspection on Critical Dimension," *CSME*, vol. 39, pp. 145-152, 2018.

Cyganek, B. and Siebert, J. P., *An Introduction to 3D Computer Vision Techniques and Algorithms*, John Wiley & Sons Ltd., UK, pp. 15-94, 2009.

Flores-Fuentes, W., Trujillo-Hernández, G., Alba-Corpus, I. Y., et al., "3D Spatial Measurement for Model Reconstruction: A Review," *Measurement*, vol. 207, no. 112321, pp. 1-54, 2023.

Han, S., Do, M. D., Kim, M., et al., "A Precise 3D Scanning Method Using Stereo Vision with Multipoint Markers for Rapid Workpiece Localization," *J. Mech. Sci. Technol.*, vol. 36, no. 12, pp. 6307-6318, 2022.

Hartley, R. and Zisserman, A., *Multiple View Geometry in Computer Vision*, Cambridge University Press, USA, pp. 237-362, 2004.

Huang, J., Wang, Z., Xue, Q., et al., "Calibration of a Camera–Projector Measurement System and Error Impact Analysis," *Meas. Sci. Technol.*, vol. 23, no. 12, pp. 1-14, 2012.

Huang, J. C., Liu, C. S., and Tsai, C. Y., "Calibration Procedure of Camera with Multifocus Zoom Lens for Three-Dimensional Scanning

System," *IEEE Access*, vol. 9, pp. 106387-106398, 2021.

Isa, M. A. and Lazoglu, I., "Design and Analysis of a 3D Laser Scanner," *Measurement*, vol. 111, pp. 122-133, 2017.

Li, D., Zhao, H., and Jiang, H., "Fast Phase-Based Stereo Matching Method for 3D Shape Measurement," in *International Symposium on Optomechatronic Technologies*, pp. 1-5, 2010.

Lin, X., Wang, J., and Lin, C., "Research on 3D Reconstruction in Binocular Stereo Vision Based on Feature Point Matching Method," in *IEEE International Conference on Information Systems and Computer Aided Education*, pp. 551-556, 2020.

Liu, C. S., Lin, J. J., and Chen, B. R., "A Novel 3D Scanning Technique for Reflective Metal Surface Based on HDR-Like Image from Pseudo Exposure Image Fusion Method," *Opt. Lasers Eng.*, vol. 168, p. 107688, 2023.

Liu, Z., Liu, X., Duan, G., et al., "Precise Pose and Radius Estimation of Circular Target Based on Binocular Vision," *Meas. Sci. Technol.*, vol. 30, no. 2, pp. 1-14, 2019.

Lowe, D. G., "Distinctive Image Features from Scale-Invariant Keypoints," *Int. J. Comput. Vis.*, vol. 60, no. 2, pp. 91-110, 2004.

Luo, Z., Zhang, K., Wang, Z., et al., "3D Pose Estimation of Large and Complicated Workpieces Based on Binocular Stereo Vision," *Applied Optics*, vol. 56, no. 24, pp. 6822-6836, 2017.

Maini, R. and Aggarwal, H., "Study and Comparison of Various Image Edge Detection Techniques," *Int. J. Image Process.*, vol. 3, no. 1, pp. 1-11, 2009.

Taryudi and Wang, M. S., "Eye to Hand Calibration Using ANFIS for Stereo Vision-Based Object Manipulation System," *Microsyst. Technol.*, vol. 24, no. 1, pp. 305-317, 2018.

Wang, Z. F. and Zheng, Z. G., "A Region Based Stereo Matching Algorithm Using Cooperative Optimization," in *IEEE Conference on Computer Vision and Pattern Recognition*, pp. 1-8, 2008.

Yang, L., Wang, B., Zhang, R., et al., "Analysis on Location Accuracy for the Binocular Stereo Vision System," *IEEE Photon. J.*, vol. 10, no. 1, pp. 1-16, 2018.

Zhang, Z., "Determining the Epipolar Geometry and Its Uncertainty: A Review," *Int. J. Comput. Vis.*, vol. 27, no. 2, pp. 161-195, 1998.

Zhu, J., Zeng, Q., Han, F., et al., "Design of Laser Scanning Binocular Stereo Vision Imaging System and Target Measurement," *Optik*, vol. 270, no. 169994, pp. 1-21, 2022.